Available online at www.sciencedirect.com
SCIENCE DIRECT®
Catalysis Today 98 (2004) 281–288
CATALYSIS TODAY
www.elsevier.com/locate/cattod

Low temperature low pressure benzene hydrogenation on Y zeolite-supported carbided molybdenum

Ângela S. Rocha[a], Victor L. T. da Silva[b], Alexandre A. Leitão[c], Marcelo H. Herbst[c], Arnaldo C. Faro Jr[a,*]

[a]*Instituto de Química, UFRJ, Ilha do Fundão, CT, bloco A, Rio de Janeiro, CEP: 21949-900, RJ, Brazil*
[b]*Departamento de Engenharia Química, IME, Praça General Tibúrcio, 80, Praia Vermelha, Rio de Janeiro, RJ, Brazil*
[c]*Instituto de Física, UFRJ, Ilha do Fundão, CT, bloco A, Rio de Janeiro, RJ, Brazil*

Available online 1 October 2004

Abstract

Carbided molybdenum catalysts supported on ultrastable Y zeolites were prepared by adsorption of molybdenum hexacarbonyl vapors at 343 K or wet point impregnation with ammonium heptamolybdate solutions, followed in both cases by temperature-programmed carburization under a 20% methane in hydrogen mixture up to 923 K. Nitrogen physical adsorption and X-ray diffraction clearly established that the zeolite structure was preserved during the carburation treatment. Chemical analysis of the catalysts evidenced that very little loss of molybdenum occurred. Despite the fact that all catalysts had similar CO chemisorption capacities, their activity varied widely. For the same silica–alumina ratio (SAR), activity increased with increasing sodium content and, for low sodium contents, with increasing SAR. When catalyst reduction was performed with pure hydrogen, the activity was about one third of the one obtained with the carburation procedure, suggesting that a carbon containing species is the active one in this reaction. Two EPR signals with $g_{\perp}$ values 1.96 and 1.98 were observed in the carburized catalysts, that may be attributed to hexa-coordinated Mo^{5+}. The second one of these signals only appears in the most active catalysts and is attributed to Mo^{5+} ions in small carbide or oxycarbide clusters.

Keywords: Molybdenum carbide; Y zeolite; Benzene hydrogenation; CO chemisorption; EPR

1. Introduction

For many years now [1], transition metal carbides, especially the molybdenum and tungsten compounds, have been investigated as possible alternatives for platinum-group metal catalysts in several reactions of interest to the oil refining industry, such as hydrocarbon hydrogenation, isomerization and hydrogenolysis and carbon monoxide hydrogenation. They have also been found active in reactions typical of transition metal sulfides, such as hydrodesulfurization (HDS) [2] and hydrodenitrogenation (HDN) [3].

In recent years, strong interest has grown in the refining industry on hydrodearomatization (HDA) processes, as a result of increasingly stringent environmental legislation with respect to aromatics content and burning quality of oil-derived fuels. Processes based on Y zeolite-supported platinum-palladium catalysts have found successful commercial application, due to the large hydrogenation activity and reasonable sulfur tolerance of these catalysts [4]. Still, platinum group metals are sensitive to poisoning by sulfur and nitrogen and a severe hydrotreating stage is required before the final HDA step.

The present work is part of a project aimed at investigating Y zeolite-supported carbided molybdenum materials as new catalysts for the hydrogenation of aromatic hydrocarbons. Unsupported transition metal carbides [5] and alumina-supported molybdenum carbide [6] have been shown before to be active in benzene hydrogenation but, to our knowledge, activity in this reaction of zeolite-supported molybdenum carbide has only been reported with catalysts also containing platinum in their composition [7]. Further-

* Corresponding author.
E-mail address: farojr@iq.ufrj.br (A.C.F. Jr).

0920-5861/$ – see front matter © 2004 Elsevier B.V. All rights reserved.
doi:10.1016/j.cattod.2004.07.041

more, the nature of the molybdenum species obtained by carburation of Y zeolite-supported molybdenum carbonyl does not appear to have been studied before.

2. Experimental

2.1. Zeolite supports

The properties of the Y zeolite supports are shown in Table 1. Zeolites Z52-9 and Z53-9 were provided by PETROBRAS R & D Centre, CENPES. Sample Z53-9 is the same as Z52-9 after exhaustive exchange with ammonium sulphate solutions in order to remove sodium and calcination to convert the ammonium form of the zeolite to its hydrogen form. Zeolite Z54-9 was obtained from Z52-9 by partial exchange with an ammonium chloride solution in order to reduce its sodium content, followed by calcination at 673 K. Samples LZ-17 and CBV-25 are commercial zeolites manufactured by Union Carbide and Zeolyst, respectively.

2.2. Preparation of the Y zeolite-supported molybdenum precursors

The adsorbed molybdenum hexacarbonyl precursors were prepared according to the method described by Zotin [8]. The selected zeolite was first dried under vacuum at 673 K for 4 h. Without further exposure to air, it was physically mixed under argon with sufficient amount of molybdenum hexacarbonyl to produce a final catalyst containing 5 wt.% molybdenum. The mixture was transferred to a Schlenk flask, which was then evacuated, closed and heated at 343 K for 16 h. Any non-adsorbed carbonyl was removed by evacuation at room temperature.

A sample was prepared by multiple incipient wetness impregnation of zeolite Z52 with ammonium heptamolybdate (AHM) solutions, followed by drying at 393 K for 2 h and calcination at 673 K for 4 h.

2.3. Catalyst activation and nomenclature

The supported-molybdenum precursors were either carburized under flow of a 20% methane in hydrogen mixture or reduced under a flow of pure hydrogen. In both cases, the temperature was linearly raised at 10 K min^{-1} to 923 K and kept at this temperature for 1.5 h.

The nomenclature adopted for the catalysts was MoX(I)/Z, where X represents the activation procedure (C for carburization and H for reduction in hydrogen), I was used only with the catalysts prepared by impregnation and Z identifies the zeolite support. Thus, MoCI/Z52 is a carburized catalyst where the molybdenum was introduced by impregnation of zeolite Z52-9, whereas MoH/Z52 was prepared by reduction of molybdenum hexacarbonyl adsorbed on the same zeolite.

Table 1
Chemical composition and surface area of the zeolites

Zeolite	SAR[a] (FTIR)	MSA[b]/m^2 g^{-1}	wt.% Na	Unit cell formula[c]
Z52-9	9.4	615	2.13	$Na_{11}H_{23}Si_{158}Al_{34}O_{384}$
Z54-9	9.4	605	0.49	$Na_{2.5}H_{31.5}Si_{158}Al_{34}O_{384}$
Z53-9	9.0	654	0.18	$NaH_{34}Si_{157}Al_{35}O_{384}$
LZ-17	17.5	686	< 0.01	$H_{20}Si_{172}Al_{20}O_{384}$
CBV-25	25.0	756	< 0.01	$H_{14}Si_{178}Al_{14}O_{384}$

[a] Framework silica/alumina ratio.
[b] Micropore surface area measured by the BET method.
[c] Determined from SAR and Na content.

2.4. Characterization

Molybdenum contents were determined colorimetrically using the thiocyanate method [9] and sodium contents by a flame-photometric method. The carbon contents and average molybdenum oxidation states (AMOS) of the catalysts were determined from the amount of CO_2 produced and the oxygen uptake during re-oxidation of the activated catalysts at 873 K under an oxygen in helium mixture. The AMOS values were calculated from the expression:

$$N = 6 - 4\left(X_{O_2} - X_C - \frac{1}{2}X_W\right)$$

where X_{O_2} is the oxygen uptake and X_C and X_W are, respectively, the amounts of CO_2 and water formed in the re-oxidation, all expressed per molybdenum atom in the sample.

Surface areas were measured in a volumetric apparatus from nitrogen adsorption isotherms at 77 K, using the BET method. Carbon monoxide chemisorption was measured in a volumetric apparatus at 308 K. The isotherms were measured at 308 K, in the 0–400 torr pressure range. Two isotherms were obtained for each sample, with intermediate evacuation for 0.5 h at the analysis temperature to remove weakly adsorbed carbon monoxide. The amount of irreversibly chemisorbed CO was obtained from subtraction of the second isotherm from the first. In all adsorption experiments, catalyst activation (carburization or reduction) were carried-out in situ.

Infrared spectra of the zeolites and of some of the carburized catalysts were obtained in a Nicolet model Magna IR 760 FTIR spectrometer, using a sample cell with CaF_2 windows. Zeolite self-supported wafers with ca. 10 mg cm^{-2} were prepared and pre-treated at 673 K for 4 h under a 10^{-5} torr vacuum before having their FTIR spectra taken at room temperature. The same IR cell was connected to a vacuum line in which molybdenum hexacarbonyl vapours were adsorbed into the zeolite at 343 K from a side arm containing a known amount of the solid compound. The sample was then carburized in the same IR cell, as described under section 2.3. The IR spectra were obtained at room-temperature.

Electron paramegnetic ressonance (EPR) spectra were recorded in a Bruker ESP-380 FT/CW spectrometer

operating at 9 GHz (X-band) and 100 kHz field modulation. All measurements were performed at room temperature in sealed evacuated Pyrex tubes, using 1.0 Gauss of amplitude modulation. In order to avoid saturation of the signal the microwave power was kept constant at 2.0 mW. Measurements of g-factors were done against DPPH standard (g = 2.0023). The carburized catalysts were transferred to the sample tubes in a dry-box under argon atmosphere. Without exposure to air, the tubes were transferred to a vacuum line, where they were evacuated and sealed.

2.5. Catalytic activity measurements

Benzene hydrogenation experiments were performed at atmospheric pressure and 363 K in a batch apparatus with external re-circulation of the gas phase. The re-circulation loop is connected to a vacuum line that can be evacuated to ca. 10^{-5} torr. Greaseless taps are used throughout the vacuum line and re-circulation loop.

About 100 mg of an adsorbed carbonyl precursor were placed in the reactor and decomposed under flow as described under 2.3. After purging with flowing hydrogen at 363 K, the reactor was isolated and the re-circulation loop was evacuated. About 1.5×10^{-3} mol benzene vapour (ca. 4.1 kPa benzene partial pressure in the re-circulation loop) was dosed into the loop. Hydrogen, together with a known amount of nitrogen as an internal standard for the chromatographic analyses, was then introduced until atmospheric pressure was reached. After homogenization, the re-circulating gas mixture was fed to the reactor and the reaction started.

Samples of the gas phase were periodically drawn to an evacuated sample loop and injected into an Hewlett Packard gas chromatograph (HP 6890 series) equipped with a methyl siloxane capillary column (100.0 m × 250 μm × 0.50 μm) and a mass-selective detector (HP 5973).

Under the applied reaction conditions, the only observed product was cyclohexane. Initial reaction rates were obtained from the slopes at zero time of benzene conversion versus time curves.

3. Results

Molybdenum contents determined in the carburized catalysts differed by less than 10% from the nominal 5 wt.% molybdenum, demonstrating that metal loss was minimal during the carburization treatment. The micropore surface areas of the catalysts were also at most 10% smaller than the ones of the respective zeolite supports, showing that the zeolite structure was preserved during molybdenum incorporation and the carburization treatment, which was confirmed by X-ray diffraction.

Fig. 1 shows the FTIR spectra of several zeolite supports and respective catalysts in the OH stretching region. The bands appearing in these spectra have been extensively

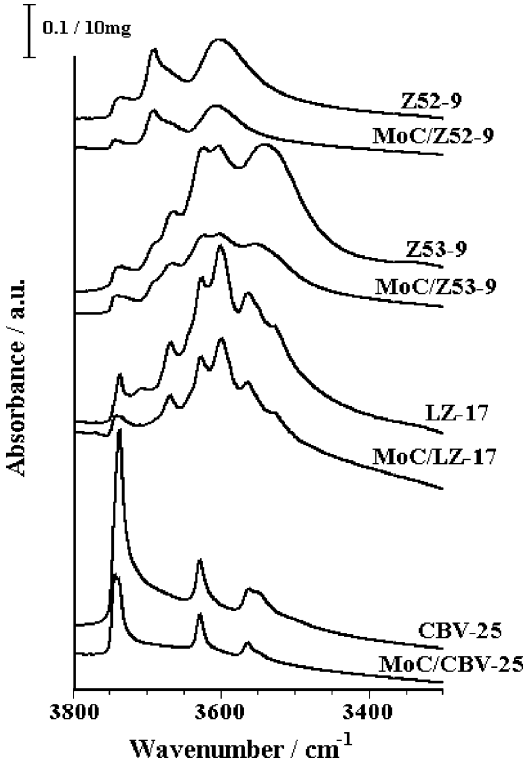

Fig. 1. FTIR spectra of zeolite supports and carburized catalysts in the OH stretching region.

discussed in the literature [10–16]. The simplest spectrum is that of zeolite CBZ-25, that displays only bands at 3739 cm^{-1}, 3630 cm^{-1} and an incompletely resolved doublet at 3564/3550 cm^{-1}. These features have been attributed respectively to silanol hydroxyl groups, bridged ≡Si(OH)Al≡ groups located in the supercages of the faujasite structure (HF bands) and bridged ≡Si(OH)Al≡ groups located in the sodalite cages (LF bands). They are typical of highly de-aluminated Y zeolites, with no extra-framework alumina (EFA).

Besides these, several other bands can be observed with zeolite LZ-17. The bands at 3607 cm^{-1} and 3539 cm^{-1} are acidic hydroxyls typical of steamed zeolites (HF′ and LF′ bands) and also respectively located in the supercages and the sodalite cages of the zeolite. The band at 3670 cm^{-1} and the small one at 3710 cm^{-1} reveal, respectively, the presence of EFA species and of a small amount of residual sodium in the zeolite.

The bands observed with zeolite Z53-9 are essentially the same as in zeolite LZ-17, although the relative intensities are different due to its lower SAR and higher Na content. The LF and LF' bands coalesced to form a broad band with an absorption maximum at 3544 cm^{-1}.

The spectrum of zeolite Z52-9 is considerably simplified, as compared to Z53-9 that was obtained from the former by ion exchange with ammonium sulphate. The band at 3692 cm^{-1}, attributed to water associated with sodium ions is prominent and the LF and HF bands cannot be discerned. The broad band at 3600 cm^{-1} has been observed with

sodium-containing zeolites and probably corresponds to non-acidic hydroxyls, since Caron et al. [10] have reported a similar band in a de-aluminated Y zeolite containing 0.3% Na that was largely unperturbed by pyridine adsorption.

In the spectra of the molybdenum-containing carburized catalysts, a general decrease in band intensities is observed, which is at least partly due to a decrease in transparency of the wafers due to their dark colour after carburization. As the number of molybdenum atoms is small as compared to the number of hydroxyl groups in the catalysts, the spectra are not very different from those of the zeolite supports. It is however clear that the LF bands suffered a stronger decrease in intensity than the remaining ones, suggesting preferential location of the carburized molybdenum at the sodalite cages. Another systematic difference was a splitting of the silanol bands, giving rise to appearance of a peak component at 3747 cm^{-1} that has been attributed to extra-framework silica species. In the present case, the appearance of this band is accompanied by a simultaneous decrease in the relative intensity of the silanol band at 3737–9 cm^{-1} and it may not be excluded that it is due to perturbation of the silanol hydroxyls by the supported molybdenum.

Table 2 summarizes the main characterization and catalytic activity results. The average molybdenum oxidation state (AMOS) values show that, in most cases, the molybdenum is in a low oxidation state after the carburization treatment. Higher AMOS values were obtained with the catalyst supported on the LZ-17 zeolite and with the catalysts supported on zeolite Z52-9 after ion exchange for sodium removal, i.e., zeolites Z53-9 and Z54-9. Therefore, higher SAR and higher sodium content favor a lower molybdenum oxidation state.

The Mo/C ratios show that considerable carbon lay-down occurred during carburization. The carbon content of the samples reduced in hydrogen was small, especially with the one prepared by impregnation (MoHI/Z52), as might have been expected from the fact that the percursor molybdenum compound, ammonium heptamolybdate, contains no carbon. A corollary is that in the sample prepared by reduction in hydrogen of the adsorbed molybdenum hexacarbonyl, some of the carbon remained in the catalyst. For the same zeolite SAR, Mo/C ratios decreased with decreasing sodium content, whereas for catalysts with low sodium content, the effect of the SAR was small. It is interesting that no Mo/C ratios lower than ca. 2, the stoichiometric ratio in β-molybdenum carbide, were obtained, which suggests that the carbon lay-down during carburization is due to formation of a carbidic species (carbide or oxycarbide) rather than to coke deposition.

The irreversible CO chemisorption capacities shown in Table 2 are seen to be very sensitive to the preparation method. The CO/Mo ratios obtained with carburization were nearly twice the ones obtained with reduction in hydrogen and the values for molybdenum incorporation by hexacarbonyl adsorption were ca. three times the ones corresponding to impregnation with AMH. In contrast, CO chemisorption capacities were remarkably insensitive to the properties of the zeolite supports. This suggests that, for the same preparation and activation methods, marked differences do not exist among the different zeolite supports in terms of dispersion or location of the supported molybdenum species. On the other hand, it is not clear whether the differences observed as a function of molybdenum incorporation and activation methods are due to differences in the nature or in the accessibility of the metal species. It is worth noticing that no irreversible CO chemisorption could be measured with the pure zeolites.

In the benzene hydrogenation reaction, the only product observed was cyclohexane. Previous results from our laboratory using a continuous flow system [17] have shown that a stable activity in this reaction is attained with catalyst at 263 K and atmospheric pressure, at least for the period of 3 h duration of the experiment. Fig. 2 shows the benzene conversion versus time curves obtained in our batch

Table 2
Catalysts carbon contents, molybdenum oxidation states, CO chemisorption capacities and catalytic activities

Catalyst	AMOS[a]	Mo/C[b]	CO/Mo[c]	Initial rate[d]/μmol s^{-1} g^{-1}	TOF[e]/s^{-1}
MoC/Z52	1.6	3.4	0.159	70	0.86
MoH/Z52	1.6	16	0.072	23	0.64
MoCI/Z52	2.2	3.8	0.049	357	14.2
MoHI/Z52	1.6	43	0.026	13	0.97
MoC/Z54	3.6	3.1	0.146	46	0.61
MoC/Z53	4.1	2.0	0.144	2.2	0.03
MoC/LZ	4.6	1.9	0.150	4.6	0.06
MoC/CBV	1.7	2.5	0.133	21	0.31

[a] Average molybdenum oxidation state obtained from oxygen uptake during reoxidation.
[b] Molybdenum to carbon ratio obtained from CO_2 produced in reoxidation.
[c] Irreversibly chemisorbed carbon monoxide to molybdenum ration.
[d] Initial rate in benzene hydrogenation at 363 K an atmospheric pressure.
[e] Same as d, expressed as turnover frequency based on CO chemisorption.

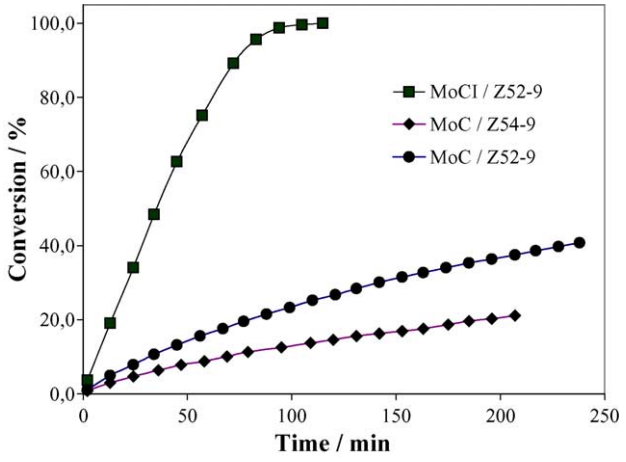

Fig. 2. Conversion vs. time curves for benzene hydrogenation at 363 K and atmospheric pressure in a batch recirculating apparatus.

recirculating reactor for some catalysts. Little decrease in the slope of these curves is observed as a function of time and the one which occurs may be chiefly attributed to the decrease in concentration of benzene in the gas phase. This is in sharp contrast with an experiment carried-out with unsupported β-molybdenum carbide, where the conversion ceased to increase after a few minutes reaction and stabilized at a low benzene conversion value (ca. 8%).

The initial rates shown in Table 2 span a large range of values. For the same zeolite SAR, catalytic activity increased with the sodium content, whereas for zeolites with a low sodium content the activity markedly increased with increasing SAR. This is the same general trend as observed with the AMOS values, although the correlation between activity and AMOS is not linear.

Catalysts reduced in hydrogen had significant activity, but the presence of methane in the activating gas caused large increases in activity, especially with the catalysts prepared by impregnation, which had by far the largest activity among all catalysts.

If the activity results are expressed in terms of turnover frequency (TOF) values, based on CO chemisorption, it is clear that the main effect of the presence of methane in the activating gas stream is to increase the number of accessible coordinatively unsaturated sites (CUS), rather than their intrinsic activity, as there was little variation in TOF values. On the other hand, the main effect of the zeolite SAR and sodium content seems to be in the quality, rather than in the number of accessible CUS.

The TOF value obtained with the carburized catalyst prepared by impregnation (MoCI/Z52) was more than one order of magnitude larger than observed with the corresponding one prepared by hexacarbonyl adsorption (MoC/Z49). Therefore it seems that the two methods of molybdenum incorporation lead to rather different supported species after carburization.

The EPR spectra of the catalysts are presented in Fig. 3 and the corresponding g-values are shown in Table 3. One

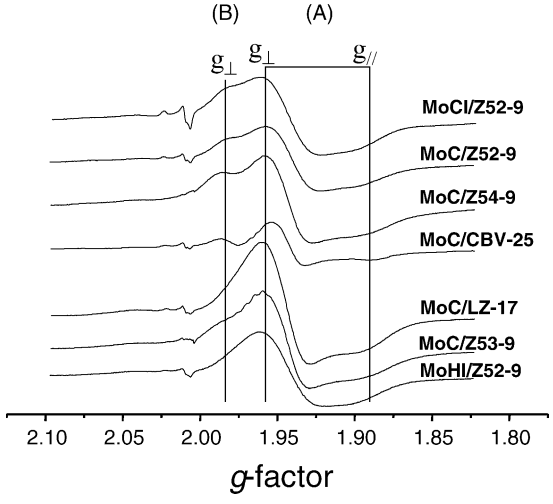

Fig. 3. EPR spectra of Y zeolite-supported catalysts after activation.

Table 3
g-Tensor values for the EPR signals observed

Catalyst	Signal A		Signal B
	$g_\perp$	$g_{//}$	$g_\perp$
MoCI/Z52	1.961	1.89	1.978
MoC/Z52	1.958	1.89	1.978
MoC/Z54	1.959	1.89	1.982
MoC/CBV	1.954	1.88	1.987
MoC/LZ	1.960	1.89	–
MoC/Z53	1.958	1.89	–
MoHI/Z52	1.961	1.90	–
5% Mo in NaY[a]	1.957	1.90	–
5% Mo in HY[b]	1.960	1.88	–

[a] Reference [10], using $Mo(CO)_6$.
[b] Reference [11], using $MoCl_2O_2$.

major signal with axial tensor components $g_\perp = 1.96$ and $g_{//} = 1.88$ (A signal) is observed in the spectra of all samples. According to previous work [18–20], this signal is assigned to Mo^{5+} as a compensation cation located at the so-called type II sites in the zeolite supercages. The very small fluctuations in the g values shown in Table 3 reflect different sample compositions and topology.

A second Mo^{5+} EPR signal with axial tensor components $g_\perp = 1.98$ and unresolved $g_{//}$ appears in some catalysts (B signal). This signal is clearly connected with catalytic activity: Table 2 shows that MoC/Z54, MoC/Z52 and MoCI/Z52 are the most active catalysts, and their EPR spectra in Fig. 3 display the most intense B signal. On the other hand, catalysts MoC/LZ-17, MoC/Z53 and MoHI/Z52, which are the least active catalysts, present no B signal or present it with much diminished intensity (MoC/Z53). Furthermore, sample MoC/CBV-25, which has an intermediate activity, presents a relatively small intensity for the B signal.

The estimated linewidth of the EPR signal of all samples is about 50 G, but signal overlapping precludes its exact determination. However, for the MoC/CVB sample the signal presents a better spectral resolution and the linewidth is about 20 G, indicating a narrower distribution of molybdenum species in zeolite CBV-25.

The spectrum of MoC/Z53 catalyst shows a well-resolved hyperfine structure in signal A, with hyperfine interaction constant of about 10 G. This hyperfine structure is induced by interaction between the unpaired electron of Mo^{5+} ions and Al^{3+} lattice ions (^{27}Al, 100% natural abundance, $I = 5/2$). This hyperfine structure is also observed, but less resolved, in the spectra of MoC/Z54 and MoC/CBV, all of which have low sodium content.

It is interesting to note that, in addition to the Mo^{5+} EPR spectra, all samples also present an anisotropic EPR signal with rhombic symmetry at $g_1 = 2.022$, $g_2 = 2.009$ and $g_3 = 2.006$, as shown in Fig. 3. This signal is assigned to O_2^- coordinated to Mo^{6+} sites (Fig. 4) [21,22]. The high value found for g_1 is consistent with a partially covalent bonding between a superoxide species and a Mo^{6+} site in the zeolite. This reveals that, despite the fact that the samples were

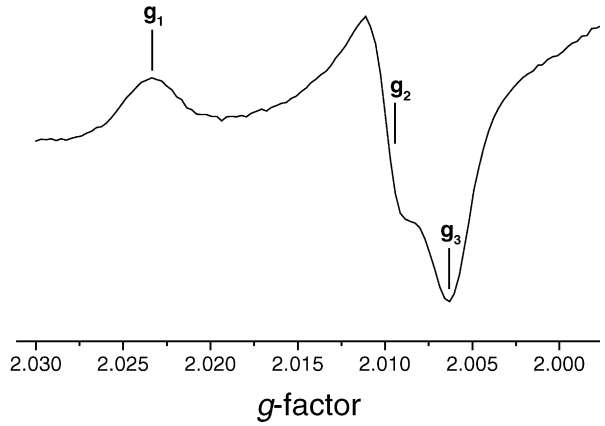

Fig. 4. Anisotropic signal in the spectra of the activated catalyts due to superoxide adsorbed on Mo^{6+}.

manipulated under argon during their transference to the EPR tubes, some exposure to oxygen could not be avoided.

The formation of carbonaceous deposits is usually observed in catalysts activated by carburization, but in this work the isotropic EPR signal caused by coke formation in $g = 2.003$, as reported by Ma et al. [23] in the reaction between Mo/ZSM-5 and CH_4, was not observed. This could be due to the activation conditions employed in this work, where the presence of hydrogen in the activating gas stream may have prevented the lay-down of coke.

4. Discussion

The first question to be addressed here is whether or not carbidic molybdenum species (carbides or oxycarbides) are formed by carburization of Y zeolite-supported molybdenum. The fact that the largest molybdenum to carbon ratios obtained were close to the stoichiometric value of two found in the β-molybdenum carbide, the fact that no EPR signal attributable to coke lay-down could be observed in the carburized catalysts, plus the fact that reduction in hydrogen led to considerably lower activity than the carburization treatment are strong indications that carbidic species are indeed formed in our catalysts.

Formation of oxycarbide nanoclusters inside NaY zeolite cages by vacuum decomposition of adsorbed molybdenum hexacarbonyl has been proposed by Iwasawa and co-workers [24–26]. With HY zeolites formation of these species is precluded due to oxidation by the zeolite protons. Our zeolites are mainly in the H form, the highest sodium content corresponding to only 1/3 of the framework aluminum sites, as shown in Table 1. Therefore, decomposition of the adsorbed hexacarbonyl cannot be the principal method of generation of carbidic species in our experiments. However, the fact that the catalyst prepared by hexacarbonyl adsorption and reduction in hydrogen has some carbon in its composition, plus the fact that its carbon content is much higher than that of the reduced catalyst prepared by impregnation of the zeolite with a carbon-free precursor suggests some contribution of this mechanism. Our carburization treatment is known to convert bulk or alumina-supported molybdenum trioxide to molybdenum carbide and most of the carbidic species in our catalysts must have been formed through this route. It is interesting to note that the catalysts supported on the zeolites with the highest protonic acidities (lowest SAR and lowest sodium contents, intense HF and LF bands in the FTIR spectra) are also the ones with the highest carbon lay-down (MoC/Z53 and MoC/LZ). The high AMOS values in these catalysts indicate that oxycarbides rather than carbides are produced in the carburization treatment.

The following sequence of reactions may explain the formation of the oxycarbide species:

(1) Decomposition of the adsorbed hexacarbonyl, as proposed by Iwasawa and co-workers [24–26]:

$$2Mo(CO)_6 \rightarrow Mo_2OC$$

(2) Oxidation of the initially formed oxycarbide by acidic protons from the zeolite framework:

$$Mo_2OC + xZOH \rightarrow 2Mo(ZO)_{x/2} + CO + x/2H_2$$

where ZOH stands for a proton attached to a zeolite framework position. This reaction must be favored in the more acidic zeolites and the resulting molybdenum species function as charge-compensating cations at the zeolite framework.

(3) Formation of oxycarbides in a range of molybdenum oxidation states by the carburization treatment:

$$Mo(ZO)_y + zCH_4 \leftrightarrow MoC_z(ZO)_{y-4z} + 4zZOH$$

This must be an equilibrium whose position depends on zeolite acidity and methane partial pressure.

(4) In the presence of hydrogen in the gas phase these reactions may compete with reduction equilibria, also dependent on zeolite acidity and partial pressure of the gases:

$$Mo(ZO)_y + xH_2 \leftrightarrow Mo(ZO)_{y-2x} + 2xZOH$$
$$MoC_z(ZO)_y + xH_2 \leftrightarrow MoC_z(ZO)_{y-2x} + 2xZOH$$
$$MoC_z(ZO)_y + xH_2 \leftrightarrow MoC_{z-x/2}(ZO)_y + x/2CH_4$$

It is not implied in these equations that the molybdenum species are necessarily monomeric, i.e. the possibility of cluster formation is not excluded. In fact the formation of metallic molybdenum clusters by reduction in hydrogen of supported molybdenum has been proposed before [24,26] and the oxycarbide produced upon decomposition of molybdenum hexacarbonyl is proposed to be a di-molybdenum species [24–26].

These equilibria may explain why more acidic zeolites tend to favor higher oxidation states for the molybdenum, while not precluding the formation of carbidic species. From the AMOS and molybdenum to carbon ratios, the average formula of the molybdenum species in our catalysts are as shown in Table 4.

Table 4
Average formula of the molybdenum species in the activated catalysts

Catalyst	Average Formula
MoC/Z52	$MoC_{0.29}(ZO)_{1.6}$
MoH/Z52	$MoC_{0.06}(ZO)_{1.6}$
MoCI/Z52	$MoC_{0.26}(ZO)_{2.2}$
MoHI/Z52	$MoC_{0.02}(ZO)_{1.6}$
MoC/Z54	$MoC_{0.32}(CO)_{3.6}$
MoC/Z53	$MoC_{0.50}(ZO)_{4.1}$
MoC/LZ	$MoC_{0.53}(ZO)_{4.3}$
MoC/CBV	$MoC_{0.40}(ZO)_{1.7}$

The catalytic activity results show that, while the presence of carbon strongly promotes activity, the catalysts containing the highest amounts of carbon are not the most active and a low molybdenum oxidation state is required for good catalytic activity. The fact that the catalyst reduced in hydrogen and prepared by adsorption of molybdenum hexacarbonyl is more active than the reduced catalyst prepared from a carbon-free precursor suggests that carbidic species are also at least partly responsible for the activity of the reduced catalysts, but it may not be completely excluded that carbon-free reduced molybdenum species are active in CO chemisorption and in benzene hydrogenation. It should be pointed-out, however, that both carbon monoxide and benzene are carbon compounds, so that formation of carbidic species upon contact of these molecules with highly reduced molybdenum atoms or, more likely, clusters is not impossible.

Apart from a signal assigned to a superoxide species in interaction with Mo^{6+}, the only paramagnetic species detected by EPR in the activated catalysts correspond to Mo^{5+}. The signal referred to here as signal A ($g_{\perp} = 1.96$) is observed in all samples and it is not clear to what extent it was produced during catalyst preparation and activation or was at least partly formed due to exposure of the activated catalysts to oxygen: the presence of the superoxide signal in all samples clearly establishes that a small exposure to oxygen did indeed occur. The conclusion that the exposure was small derives from the very small intensity of this signal.

The A signal is assigned to hexacoordinated Mo^{5+} species as charge compensating cations located at type II sites in the faujasite supercages. Its formation therefore requires the existence aluminum exchange sites of the zeolite structure and must be disfavored by increases in SAR and sodium content. Carbon is not required for its formation, since it also occurs with the carbon-free reduced catalyst MoHI/Z52. It is worth noticing that the A signal in the least active of all catalysts, MoC/Z53, displayed a clear hyperfine structure indicative of Mo^{5+}-Al^{3+} interaction, which is not observed with the other supports derived from the same zeolite but with higher sodium content. This is consistent with the location of molybdenum ions predominantly as charge compensating cations in the zeolite framework in MoC/Z53 and strongly indicates that these molybdenum ions are inactive in the benzene hydrogenation reaction.

Signal B, on the other hand, has larger *g*-values, which may result from differences in the number or in the nature of the ligands around the central Mo^{5+} atom. It appears to have some correlation with catalytic activity, but the species responsible for its existence cannot be the active site for benzene hydrogenation, since it was largest in the carburized catalysts with the lowest molybdenum oxidation state. It may however derive from exposure to oxygen of the active sites. Carbon is required for the formation of this species, since it is not observed with MoHI/Z52. This is consistent with its larger *g*-value, as carbide is a weaker ligand than oxide. It is favored by larger SAR values and sodium contents and is therefore probably not associated with the aluminum exchange sites of the zeolite. Thus, one distinct possibility for this species is that it derives from carbide or oxycarbide nanoclusters adsorbed on the supercage walls, by exposure to oxygen.

The very large activity of the carburized catalyst prepared by impregnation with AHM remains to be explained. It is generally accepted that impregnation with AHM does not result in molybdenum deposition in the zeolite cages, since heptamolybdate is an anion and Y zeolites are cation exchangers. It is not impossible, however that molybdenum migrates to the zeolite cages during high temperature treatments, especially calcination due to the volatility of molybdenum trioxide, but it is expected that the molybdenum distribution is less homogeneous than in the case of hexacarbonyl adsorption, resulting in the presence of several molybdenum atoms per supercage located near to the external surface of the zeolite crystals, even for low molybdenum contents. Carburization of these species should result in larger carbide nanoclusters, which would explain the lower CO chemisorption capacity of this catalyst as compared to the one prepared by carburization of the adsorbed hexacarbonyl. A higher intrinsic activity of the molybdenum sites at the surface of these clusters, as compared to more dispersed species has to be assumed.

We do not believe that the molybdenum is predominantly located at the external surface of the zeolite crystals in the catalyst prepared by AHM impregnation. If this was the case, a very low dispersion of the carburized molybdenum would be expected and the bulk carbide proved to be a very unstable catalyst for benzene hydrogenation under our conditions.

Another important difference between the catalyst prepared by impregnation with AHM and the ones prepared by hexacarbonyl adsorption is that solid state ^{27}Al NMR results to be presented elsewhere [27] clearly showed the existence of aluminum molybdate in the calcined precursor of the former. This must have resulted from reaction of molybdenum trioxide with extraframework aluminum and may have helped to minimize the formation during carburization of the inactive charge compensating species responsible for the A signal in the EPR spectra.

It is worth pointing-out that the A signal in the EPR spectra of the samples prepared by AHM impregnation (MoCI/Z52 and MoHI/Z52) occurs at a $g_{\perp}$ value (1.961) slightly different from the ones observed with samples

prepared by the hexacarbonyl adsorption method (< 1.960), as shown in Table 3. This is an indication of some difference in the nature of the species responsible for this signal, probably related to its location at the zeolite structure.

5. Conclusions

Catalysts prepared by carburization of molybdenum supported on ultrastable Y zeolites proved to be active in benzene hydrogenation at 363 K and atmospheric pressure. The activities of the carburized catalysts were much higher than those of catalysts obtained by reduction in hydrogen of the same precursors. Catalytic activity was favored by increasing SAR and sodium content of the zeolite supports. The same factors favored the production of highly reduced molybdenum species during carburization. Thus benzene hydrogenation in these catalysts seems to occur on highly reduced carbon-containing molybdenum species.

EPR spectra obtained after exposure of the activated catalysts to a small amount of oxygen revealed two signals attributed to paramagnetic Mo^{5+} species, one of which seemed to have some correlation with catalytic activity. This signal is tentatively assigned to molybdenum carbide or oxycarbide nanoclusters, active in benzene hydrogenation, after exposure to oxygen.

A carburized catalyst where the molybdenum was introduced by impregnation with ammonium haptamolybdate solution was much more active than the ones prepared by carburization of adsorbed molybdenum hexacarbonyl, despite having a lower carbon monoxide chemisorption capacity. It is hypothesized that this is due to formation of larger carbide or oxycarbide nanoclusters in the former. Molybdenum ions at aluminum sites in the zeolite framework are thought to be inactive in the benzene hydrogenation reaction.

Acknowledgements

This project was finantially supported by FINEP through the Fundo Setorial CTPETRO and by PETROBRAS. A.S.R. thanks the Agência Nacional do Petróleo for a doctorate scholarship.

References

[1] R.B. Levy, M. Boudart, Science 181 (1973) 547.
[2] J.S. Lee, M. Boudart, Appl. Cat. 19 (1985) 207.
[3] S.Z. Li, J.S. Lee, T. Hyeon, K.S. Suslick, Appl. Cat. A 184 (1999) 1.
[4] A.J. Suchanek, Oil Gas J. 88 (1990) 109.
[5] C. Marquez Alvarez, J.B. Claridge, A.P.E. York, J. Sloan, M.L.H. Green, Stud. Surf. Sci. Catal. 106 (1997) 485.
[6] J.S. Lee, M.H. Yeomk, K.Y. Park, I. Nam, J.S. Chung, Y.G. Kim, S.H. Moon, J. Catal. 128 (1991) 126.
[7] T. Bécue, J.M. Manol, C. Potvin, R.J. Davis, G. Djéga-Mariadassou, J. Catal. 186 (1999) 110.
[8] J.L. Zotin, These du Doctorat, Universite Claude Bernard Lyon I, Lyon, 1993.
[9] G.H. Jeffrey, J. Bassett, J. Mendham, R.C. Denney, Vogel - Análise Química Quantitativa, Livros Técnicos e Científicos Editora S.A., São Paulo, 1992.
[10] O. Cairon, K. Thomas, A. Chambellan, T. Chevreau, Appl. Catal. A: General 238 (2003) 167.
[11] S. Khabtou, T. Chevreau, J.C. Lavalley, Micropor. Mater. 3 (1994) 133.
[12] M.A. Makarova, J. Dwyer, J. Phys. Chem. 97 (1993) 6337.
[13] O. Cairon, S. Sellem, C. Potvin, J.M. Manoli, T. Chevreau, in: L. Bonneviot, S. Kaliaguine (Eds.), Zeolites, A Refined Tool for Designing Catalytic sites, Studies in Surface Science and Catalysis, vol. 97, Elsevier, Amsterdam, 1995, p. 513.
[14] L.M. Kustov, V.B. Kazansky, S. Beran, L. Kubelkova, P. Jiru, J. Phys. Chem. 91 (1987) 5247.
[15] A. Zecchina, S. Bordiga, G. Spoto, D. Scarano, G. Petrini, G. Leofanti, M. Padovan, C. Otero Aeran, J. Chem. Soc. Faraday Trans. 88 (1992) 2959.
[16] C. Carvajal, P.J. Chu, J.H. Lunsford, J. Catal. 125 (1990) 123.
[17] A. Rocha, A.C. Jr Faro, V.T. Silva, XVII Ibero-American Symposium on Catalysis, Isla de Margarita, 2002.
[18] S. Abdo, R.F. Howe, J. Phys. Chem. 87 (1983) 1722.
[19] H. Minming, R.F. Howe, J. Catal. 108 (1987) 283.
[20] J.L.G. Fierro, J.C. Conesa, A.L. Agudo, J. Catal. 108 (1987) 334.
[21] M. Huang, J. Yao, S. Xu, Ch. Meng, Zeolites 12 (1992) 810.
[22] H. Min-Ming, J.R. Johns, R.F. Howe, J. Phys. Chem. 92 (1988) 1291.
[23] D. Ma, Y. Shu, X. Bao, Y. Xu, J. Catal. 189 (2000) 314.
[24] T. Shido, K. Asakura, Y. Noguchi, Y. Iwasawa, Appl. Cat. A 194–195 (2000) 365.
[25] A. Yamaguchi, A. Suzuki, T. Shido, Y. Inada, K. Asakura, M. Nomura, Y. Iwasawa, J. Phys. Chem. B 106 (2002) 2415.
[26] K. Asakura, Y. Noguchi, Y. Iwasawa, J. Phys. Chem. B 103 (1999) 1058.
[27] A. Rocha, A.C. Faro Jr., V.T. Silva, (in preparation).